Naval Research Laboratory
Washington, DC 20375-5320

NRL/6850/MR—2022/1

Epitaxial Growth and Characterization of Cubic Boron Nitride

DR. DAVID F. STORM

DR. NEERAJ NEPAL

Electromagnetics Technology Branch
Electronics Science and Technology Division

DR. SERGEY I. MAXIMENKO

Quantum & Optoelectronics Branch
Electronics Science and Technology Division

DR. ANDREW C. LANG

Materials & Sensors Branch
Materials Science and Technology Division

DR. TATYANA FEYGELSON

DR. BRADFORD B. PATE

Surface Chemistry Branch
Chemistry Division

April 27, 2022

REPORT DOCUMENTATION PAGE

Form Approved
OMB No. 0704-0188

1. REPORT DATE *(DD-MM-YYYY)*	**2. REPORT TYPE**	**3. DATES COVERED** *(From - To)*
27-04-2022	NRL Memorandum Report	24 July 2019 – 15 March 2022

4. TITLE AND SUBTITLE

Epitaxial Growth and Characterization of Cubic Boron Nitride

5a. CONTRACT NUMBER

5b. GRANT NUMBER

5c. PROGRAM ELEMENT NUMBER

6. AUTHOR(S)

David F. Storm, Sergey I. Maximenko, Andrew C. Lang, Neeraj Nepal, Tatyana Feygelson, and Bradford B. Pate

5d. PROJECT NUMBER

5e. TASK NUMBER

5f. WORK UNIT NUMBER
1P56

7. PERFORMING ORGANIZATION NAME(S) AND ADDRESS(ES)

Naval Research Laboratory
4555 Overlook Avenue, SW
Washington, DC 20375-5320

8. PERFORMING ORGANIZATION REPORT NUMBER

NRL/6850/MR--2022/1

9. SPONSORING / MONITORING AGENCY NAME(S) AND ADDRESS(ES)

Air Force Office of Scientific Research
Dr. Ken Goretta, Program Officer
875 North Randolph Street, Suite 325,
Arlington, VA 22203-1995

10. SPONSOR / MONITOR'S ACRONYM(S)

AFOSR

11. SPONSOR / MONITOR'S REPORT NUMBER(S)

12. DISTRIBUTION / AVAILABILITY STATEMENT

DISTRIBUTION STATEMENT A: Approved for public release; distribution is unlimited.

13. SUPPLEMENTARY NOTES

14. ABSTRACT

Cubic boron nitride is a promising material for high power and high temperature electronic devices owing to its large band gap (~6.4 eV) and high thermal conductivity. We report here on the growth of epitaxial films of undoped and Si-doped c-BN on diamond substrates by ion beam-assisted MBE and their characterization by scanning TEM, FTIR, XPS, AFM, and Hall effect transport measurements. In addition, we report on the role that trace amounts of Mg plays in enabling the growth of c-BN.

15. SUBJECT TERMS

16. SECURITY CLASSIFICATION OF:			**17. LIMITATION OF ABSTRACT**	**18. NUMBER OF PAGES**	**19a. NAME OF RESPONSIBLE PERSON**
					Dr. David Storm
a. REPORT	**b. ABSTRACT**	**c. THIS PAGE**	U	18	**19b. TELEPHONE NUMBER** *(include area code)*
U	U	U			(202) 404-4618

Standard Form 298 (Rev. 8-98)
Prescribed by ANSI Std. Z39.18

This page intentionally left blank.

EXECUTIVE SUMMARY

Epitaxial films of cubic boron nitride are grown by ion beam-assisted molecular beam epitaxy. Scanning transmission electron microscopy confirms epitaxial BN growth with >99% cubic phase content. Trace amounts of Mg are observed to facilitate epitaxial growth of c-BN.

This page intentionally left blank.

ABSTRACT

Cubic boron nitride is a promising material for high power and high temperature electronic devices owing to its large band gap (~6.4 eV) and high thermal conductivity. However, it is the least mature of the ultrawide bandgap materials due to the lack of large-area native substrates and the difficulty of depositing epitaxial films of sufficient quality for electronic applications. We report here on the growth of epitaxial films of undoped c-BN on diamond substrates by ion beam-assisted molecular beam epitaxy and their characterization by scanning transmission electron microscopy, Fourier transform infrared spectroscopy, x-ray photoelectron spectroscopy, and atomic force microscopy. In addition, we report on the role that trace amounts of Mg plays in enabling the growth of c-BN.

OBJECTIVE

The objective of this effort is to investigate the epitaxial growth and properties of cubic boron nitride (c-BN). Undoped c-BN; Si-, Be-, and Mg-doped c-BN; and simple cubic boron nitride-based electronic devices (e.g. *p-n* diode) will be grown by ion beam-assisted molecular beam epitaxy, and the structural, electrical, and optical properties will be characterized and correlated to growth parameters such as growth rate, growth temperature, V/III ratio, etc. This effort will lead to greater understanding of the mechanisms by which high-quality c-BN can be grown and an enhancement of the DoD's ability to utilize c-BN for next generation high power and high frequency electronic devices.

Manuscript approved April 27, 2022.

BACKGROUND

Cubic boron nitride has two to four times the thermal conductivity of SiC, and five to ten times that of GaN; only diamond has a higher thermal conductivity. It has electrical properties similar to those of diamond, but candidate dopants have lower activation energies in c-BN than in diamond. For example, the activation energy of Si in c-BN is ~400 meV [1] compared to 1.7 eV for N in diamond [2], while the activation energy of Be in c-BN is ~200 meV [3] compared to 370 meV for B in diamond [2]. This suggests that *n*- and *p*- type doping in thin films is more easily attainable in c-BN than in diamond. Indeed, the first reported c-BN *p*-*n* junction device utilized beryllium and silicon as acceptors and donors, respectively [4]; it exhibited good rectifying characteristics at room temperature and operated up to 530 C [4] as shown in Fig. 1. The device was grown using the high pressure and high temperature (HPHT) method, in which a 0.5 mm-thick *n*-type c-BN layer was grown epitaxially on a *p*-type seed crystal at a pressure of 55 kBars and a temperature of ~1700 C.

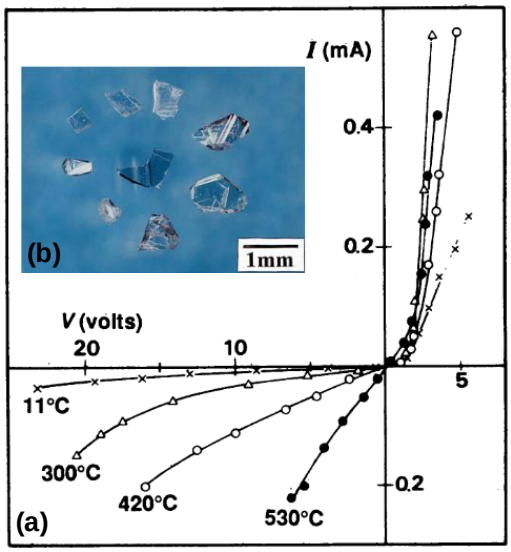

Fig. 1: (a) Temperature dependent I-V characteristics of c-BN p-n junction grown by HPHT [4] and (b) typical HPHT grown c-BN bulk crystals [11].

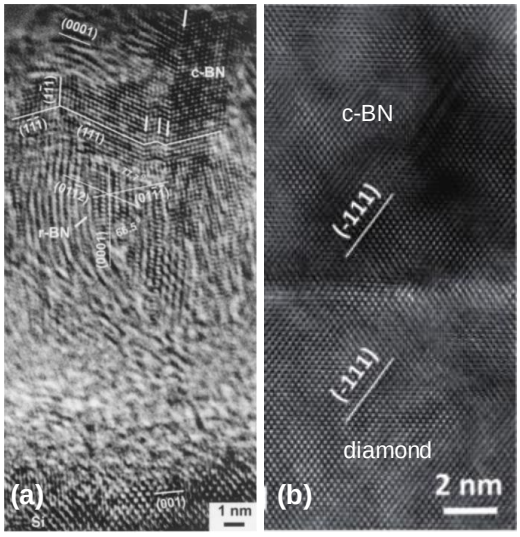

Fig. 2: Cross-sectional HRTEM images of (a) epitaxially grown c-BN with inclusions of interlayer of t-BN by IBAD [7] and (b) ion beam assisted MBE on diamond without presence of non-cubic phases [9].

Up to the present, reported sizes of bulk crystal c-BN grown by the HPHT method are in the range of a few millimeters [5, 6], too small to use for substrates (Fig. 1). Hence practical investigations of epitaxial c-BN will rely on non-native substrates, such as diamond, with which it is very nearly lattice-matched (Δa / a ~ 1%), shares a similarly high thermal conductivity, and is isoelectronic, which allows formation of heterostructures. Since the growth of epitaxial c-BN films on diamond substrates by HPHT is impractical, the heteroepitaxial growth of c-BN thin films on diamond at low pressure using ion beam assistance is currently being explored. The ion beam assist is required for growth of c-BN, likely by supplying the kinetic energy required to convert the h-BN to the metastable cubic phase. Several ion beam assisted techniques were tested to grow cubic phase BN; physical vapor deposition (PVD), plasma-enhanced chemical vapor deposition (CVD) and ion beam assisted deposition (IBAD) [7]. The resulting film

quality is typically unacceptable for electronic applications due to the build-up of strong compressive stress, inclusions of h-BN, turbostratic t-BN (disordered *h*-BN) interlayers, and polycrystalline structure as shown in Fig. 2. However, heteroepitaxial growth of single domain pure c-BN on diamond substrates by ion beam assisted MBE system was recently demonstrated [8, 9] (Fig. 2[b]).

Reliable doping of c-BN is problematic, however. Reported values of electron and hole concentrations with dopant used are summarized in Table 1. To date there are few reports of successful *n*-type doping in MBE-grown c-BN, and none as yet of successful *p*-type doping.

Table 1: Doping and electrical properties of c-BN [1, 3, 10-13].

Dopant (Conductivity type)	**Resistivity, [Ω -cm]**	**Carrier Concentration, [cm^{-3}]**	**Activation Energy, [eV]**
S (n)	20000	$2x10^{14}$ - $7.5x10^{19}$	0.18 - 0.32
C (n)	-	-	0.28 - 0.41
Si (n)	0.1-1000	$1x10^{13}$ - $5x10^{20}$	0.24
Be (p)	0.35 – 10	$3x10^{17}$ - $6x10^{18}$	0.19 - 0.24
Zn (p)	~100		0.1 - 0.3
Mg (p)	0.1 – 5000	$4x10^{14}$ – $1x10^{18}$	0.1 - 0.3

TECHNICAL APPROACH

Ion beam-assisted molecular beam epitaxy is used to grow films of c-BN on (100) diamond substrates. Diamond is an attractive substrate material as it possesses a cubic crystal structure, is isoelectronic to c-BN, and is nearly lattice-matched to c-BN (~1.3% lattice mismatch). Additionally, like c-BN, diamond has an ultrawide bandgap (5.5 eV) and high thermal conductivity, the highest found in nature. Thus, c-BN/diamond heterostructures hold great promise for high power, high temperature electronic devices.

Molecular beam epitaxy is advantageous for growing electronic devices and layer structures due to the extremely high purity with which material can be deposited, the tight control over layer thicknesses, and the formation of hyperabrupt interfaces. Low impurity incorporation and epitaxial growth reduce scattering from impurity atoms and grain boundaries, improving carrier mobility.

Ion beam assistance during vapor-phase growth is universally recognized to be a critical contributor to the formation of cubic BN, which is thermodynamically metastable under typical vapor phase growth pressures and temperatures.

NRL's MBE deposition chamber is equipped (Fig. 3) with a 6-pocket electron beam evaporator for the evaporation of elemental boron; a Veeco Uni-Bulb rf-plasma source for supplying "activated" nitrogen (N*) and which has been used extensively in the epitaxial growth of gallium nitride and related materials; a Mantis RFMAX30 ion source providing energetic ions of a continuously variable mixture of Ar and N_2, standard single- and dual-filament effusion cells for depositing group-III metals (Ga, Al, In) and dopants (Si, Be, and Mg); reflection high energy electron diffraction (RHEED), and a quartz crystal microbalance (QCM). The substrate temperature was monitored by a thermocouple.

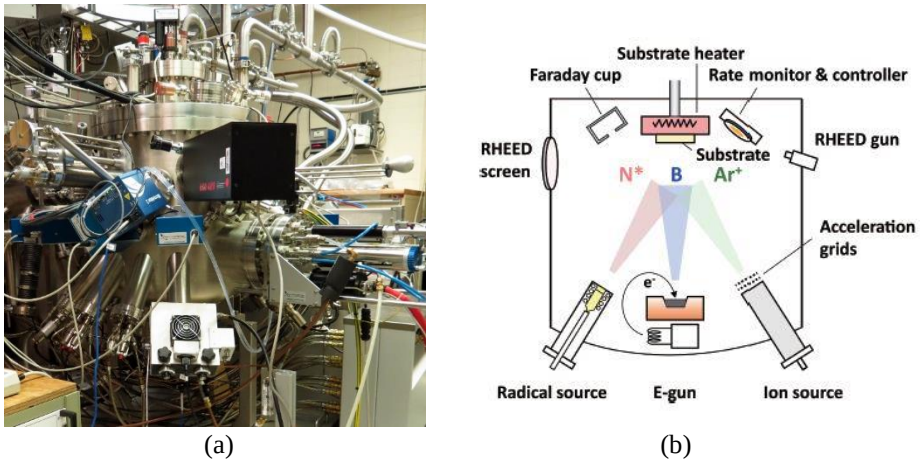

(a) (b)

Fig. 3. (a) NRL's custom-built MBE deposition chamber and (b) a schematic representation of the main components of an ion beam-assisted MBE system (Ref. 9).

The diamond substrates upon which c-BN has been grown were commercially obtained synthetic, single-crystal, CVD IIa type, (001)-oriented wafers. Crystalline quality of the selected substrates was evaluated through selective defect etch by oxygen plasma RIE process [14] as shown in Fig. 4. Dislocation density was estimated of about 10^6 cm^{-2}. The as-received wafers were finished with a "basic polish", which resulted in a root-mean-square roughness of ~5 nm, as measured by atomic force microscopy (AFM). Several of the as-received wafers were sent to an external vendor for chemical-mechanical polishing (CMP), which reduced the rms roughness measured by AFM to ~0.5 nm (Fig. 5).

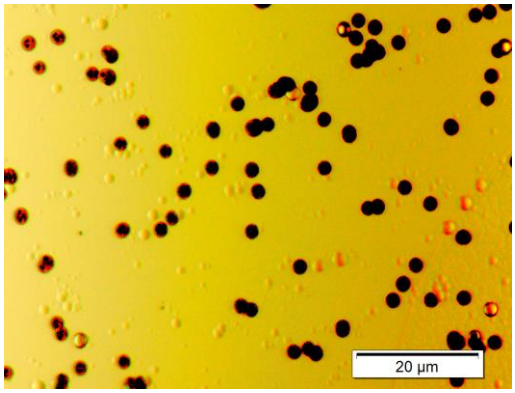

Fig. 4: Optical image of IIa (100) diamond CVD substrate surface with dislocation etch pits formed after oxygen plasma RIE process.

The CMP wafers were acid cleaned by boiling in mixture of fuming nitric acid and sulfuric acid (60% HNO_3, 40% H_2SO_4) followed by boiling in aqua regia, a dip in 10% HF, a deionized water rinse, and finally a rinse in ethanol. Acid treatments (such as that used here) of diamond

(100) surfaces are known to preserve near surface atomic order and to leave the surface oxygen terminated [15]. After acid cleaning, the wafers were loaded into the UHV environment with no further surface preparation.

Growth of c-BN was achieved on both the solvent-cleaned and the CMP wafers. This suggests that c-BN growth does not depend sensitively on the details of the diamond substrate surface.

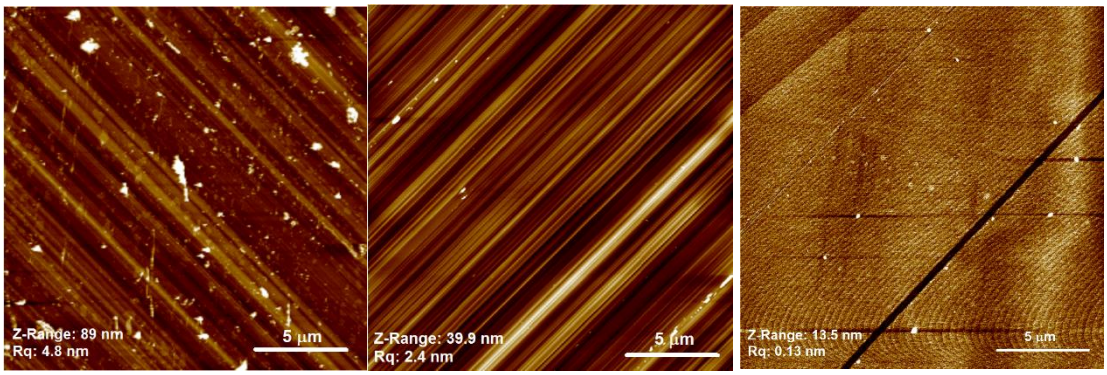

Fig. 5. AFM images of as-received (left), solvent cleaned (center), and CMP surfaces of commercial diamond substrates. The z-range and rms roughness is indicated on each image. The field of view of all images is 20 × 20 μm^2.

To date, each c-BN growth has proceeded under conditions of constant substrate temperature, N* flux, Ar ion flux, although these conditions may change between growths. All growths thus far have employed a N* flux of ~2.2×10^{14} $cm^{-2}s^{-1}$; substrate temperatures during growth have ranged from 650 C to 850 C. Ar ion fluxes are estimated at ~7×10^{14} $cm^{-2}s^{-1}$. Film growth temperatures were 850 C on the as-received diamond wafers, and either 850 C or 700 C on the CMP wafers, as shown in Table 2.

The samples were characterized by Fourier transform infrared (FTIR) spectroscopy, x-ray photoelectron spectroscopy (XPS), transmission electron microscopy (TEM) and electron energy loss spectroscopy (EELS).

TECHNICAL PROGRESS

Progress Made

Growth of c-BN on Diamond

We have grown c-BN layers on diamond (100) substrates, and in the course of this program we have discovered that trace amounts of magnesium facilitate c-BN growth, described in more

detail below and in Reference 16. A characteristic image of a diamond (100) substrate with an epitaxially grown BN film is shown in Fig. 6.

Scanning transmission electron microscopy (STEM) of a recent sample revealed an epitaxial and highly textured film composed of at least 99% cubic BN on the diamond substrate. STEM imaging confirms that the c-BN layer has been grown on the (100) surface plane of the diamond and adopts the same orientation as the diamond substrate. This can be visually confirmed in the STEM image in Figure 7a: the inset fast-Fourier transforms (FFTs) from the image show the electron beam is oriented along the [110] in both the diamond and c-BN with the (001) plane perpendicular to the growth direction of the c-BN layer, as denoted by the position of the 002 spot in the inset FFT. Imaging also reveals the presence of a high density of stacking faults, which appear in the image as diagonal features inclined 55° to the growth plane The interface between the diamond and the c-BN film appeared structurally abrupt, and was confirmed by electron energy loss spectroscopy (EELS). There is no indication of an interfacial layer between the diamond substrate and c-BN film. While the film is epitaxial, a high density of stacking faults, indicative of twinning, are clearly visible in the micrographs (Fig. 7) as diagonal features inclined 55° to the growth plane. These stacking faults comprise nearly all of the visible defects, though isolated misfit dislocations appear as vertical streaks and contrast near the interface between the diamond and c-BN layer.

Fig. 6: Optical image of BN film grown on 6x6 mm^2 diamond IIa (100) CVD substrate. H-BN and c-BN are distinguished by color. H-BN films are grey color as shown in the image, while c-BN films are colorless and undistinguished from diamond substrate. Corner features are footprint of MBE sample holder.

A small "pre-peak" feature ~191.3 eV is found in the energy loss spectra from the interface, surface, and isolated regions in the bulk of the c-BN film. This pre-peak feature is attributed to a bound exciton originating from the π* orbital [17, 18] and is absent in c-BN (Fig. 7), as π* states are absent in the cubic phase due to bond hybridization. A pre-peak feature has been observed in h-BN, but the intensity is typically comparable to the main edge feature ~197 eV. Its presence in this case is suggestive of sp^2-bonded BN rather than pure h-BN, particularly since imaging does not identify any obvious hexagonal stacking within the c-BN film. This suggests that while the film is >99% cubic, consistent with the results of FTIR, very thin layers of sp^2-bonded BN appear at the surface of the film, the interface between the film and substrate, and in isolated regions of the c-BN. The presence of this feature near the film surface is not surprising as c-BN films are thought to be capped by an ultra-thin h-BN-like layer.

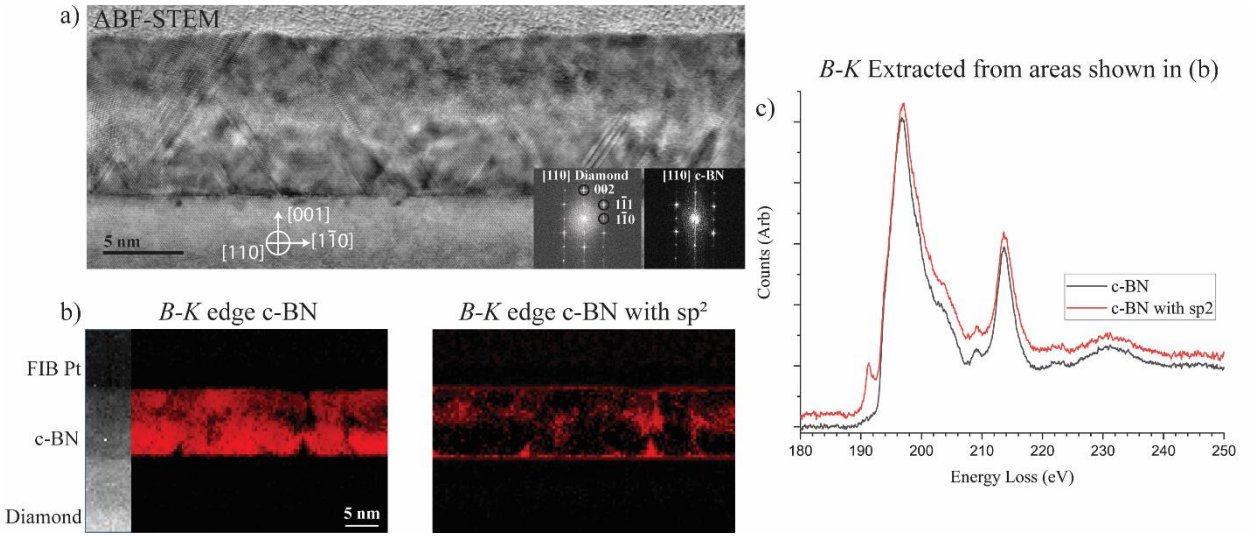

Fig. 7: Cross-sectional STEM analysis of c-BN. a) Annular bright-field STEM image of the c-BN thin film with inset FFTs from both the c-BN and diamond layers indicating the orientation of the heterostructure with respect to the electron beam. b) EELS maps showing where individual spectra features of the B K-edge are observed; left, typical c-BN spectra; right, c-BN spectra with a pre-peak feature at 191eV, indicative of the presence of some sp^2 bonding in the BN. c) The extracted EEL spectra used to form the images in b, note the red spectra has an extra pre-peak feature at 191eV. The EEL spectra in (c) were processed with a power law background subtraction and offset for visual clarity [Ref. 16].

Correlation of RHEED with BN phase

A streaked RHEED pattern arises from a smooth, epitaxial surface, while a spotty pattern indicates some roughness to the surface, and arcs indicate a polycrystalline surface. We have observed distinct RHEED patterns from the growth surfaces of c-BN and h-BN layers on diamond substrates. The RHEED pattern of a c-BN surface is characterized by broadened streaks or elongated spots, whereas an arc pattern is indicative of h-BN growth as shown in Fig. 8. This allows us to monitor the phase of the growing BN layer in real time. If the RHEED pattern indicates the loss of significant cubic character in the growth surface, either by dimming of the c-BN RHEED spots or the appearance of h-BN arcs, the growth can be temporarily halted by interrupting the boron flux until the c-BN pattern returns. A series of RHEED images from the growth of a c-BN layer during which a growth interrupt was used is shown in the Fig. 9.

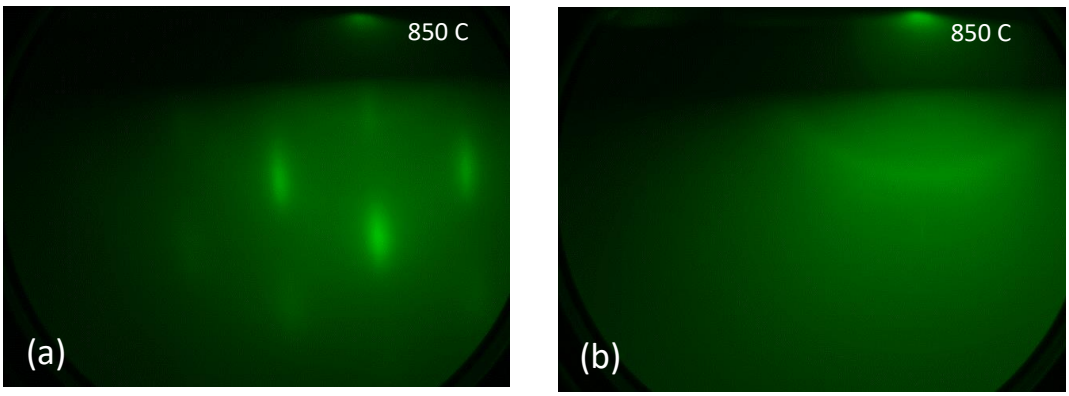

Fig. 8. RHEED images depicting patterns from a cubic BN surface (left) and a hexagonal BN surface (right). Note the elongated spots in the image at left and the arcs in the image at right.

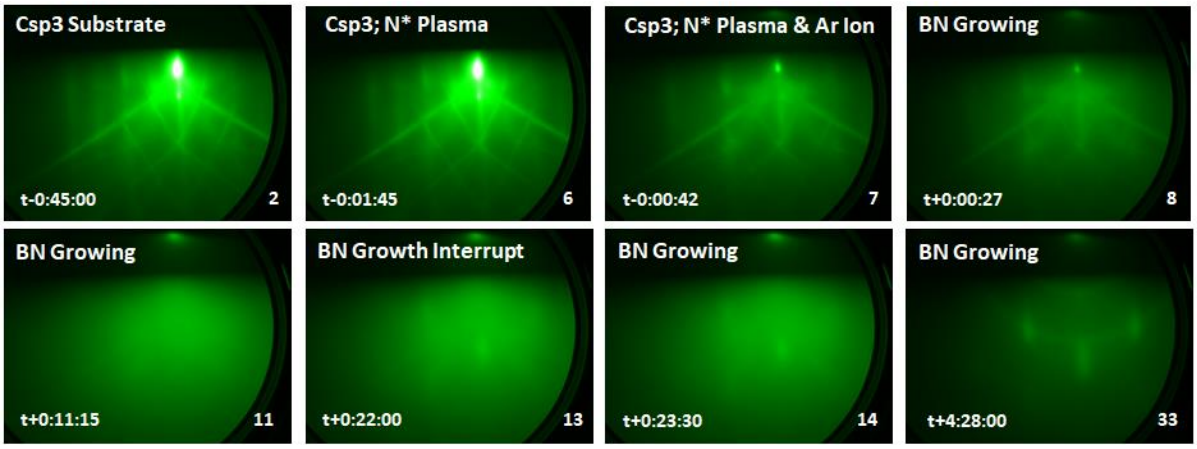

Fig. 9. RHEED images from various stages in the growth of a c-BN layer. Each image displays a short description at the top, the image number at lower right, and the time relative to the initiation of growth at which the image was taken. Note that in image 8 the RHEED pattern from the diamond substrate has dimmed significantly compared to the earlier images, since the growth of BN has begun. By image 11 there is no clear RHEED pattern. At this point the growth was interrupted by interrupting the B flux. A c-BN pattern emerged during the interrupt and is visible in image 13. The growth was resumed, and the c-BN pattern is visible shortly thereafter in image 14 as well as near the end of growth in image 33 [Ref. 16].

Observation of Mg-enabled c-BN Growth

We have observed a robust correlation between the state or recent history of the Mg cell on our MBE system and the growth of c-BN on diamond. BN films grown with the Mg effusion cell at elevated temperature, sufficient to produce a Mg flux of ~8×10^{10} $cm^{-2}s^{-1}$, but with the shutter closed, or soon after the Mg cell was used for a Mg-doped layer growth, were found to be

cubic, while BN films grown with the Mg cell at its idling temperature or long after the Mg cell had been used were hexagonal, as shown in Table 2.

Table 2. Sample ID, boron nitride phase (determined by FTIR), diamond substrate surface finish and preparation, film growth temperature, state of Mg cell during growth, and the number of previous samples since the Mg effusion cell had been used during a film growth.

Sample ID	BN Phase	Diamond Surface Pre-Treatment	T_{Sub} (°C)	Mg cell	Samples since Mg use
1A	Hex	CMP + Acid Clean	850	Idle	224
1B	Cubic	CMP + Acid Clean	850	Hot	225
1C	Cubic	CMP + Acid Clean	850	Hot	226
2A	n/a	CMP + Acid Clean	700	Idle	188
2B	Cubic	CMP + Acid Clean	700	Hot	189
2C	Hex	CMP + Acid Clean	700	Idle	190
3A	Hex	As-received; Solvent degrease	700	Idle	77
3B	Mix	As-received; Solvent degrease	700	Idle	1
3C	Mix	As-received; Solvent degrease	700	Idle	2

Three series of three samples were grown in which one or two samples in each series were unintentionally exposed to a very small flux of Mg, while the rest were not, as shown in Table 2. In each instance in which the substrate was exposed to even a trace amount of Mg, FTIR indicated the sample to be phase-pure c-BN, whereas those samples which were not so exposed were either phase-pure h-BN or the sample was too thin to make a clear determination.

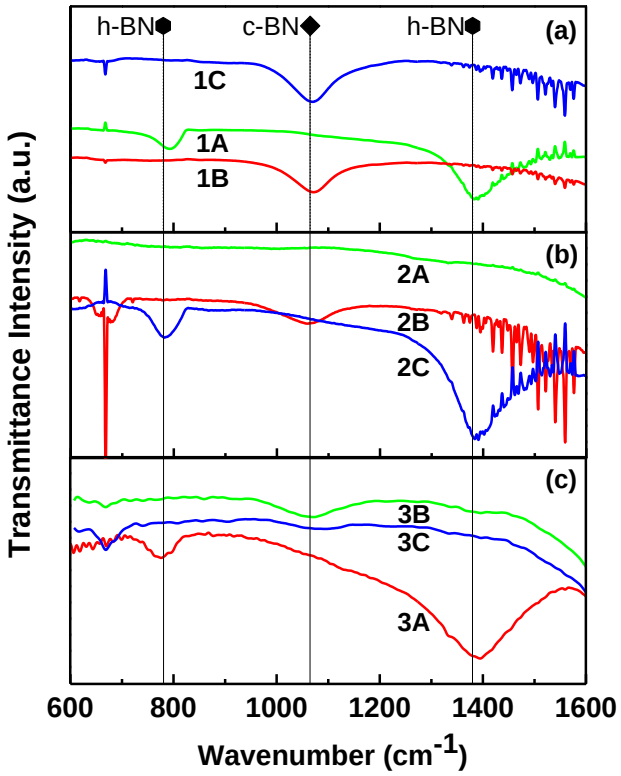

Fig. 10: FTIR spectra of the nine samples enumerated in Table 2. Signatures of c-BN are clearly visible in the spectra of Samples 1B, 1C, 2B, and 3B. The spectrum of Sample 3C, which was grown immediately after 3B, exhibits a weak c-BN signal with a possible h-BN component. FTIR spectra of samples 1A, 2C, and 3A exhibit clear signatures of h-BN, while Sample 3B appears to exhibit a weak h-BN component combined with a clear c-BN signal. Sample 2A is too thin for features of either phase to appear, but XPS analysis suggests that the BN film is sp^2-bonded [Ref. 16].

All films were characterized by FTIR, and the results are shown in Fig. 10. In most cases the films appeared to be phase-pure: either completely cubic or completely hexagonal. Two samples, 3B and 3C, appeared to have mixed phases: Sample 3B appeared to be predominantly c-BN with a small h-BN component, while Sample 3C exhibited a weak c-BN signal possibly combined with an even weaker h-BN signal. Another sample, 2A, did not show evidence of either

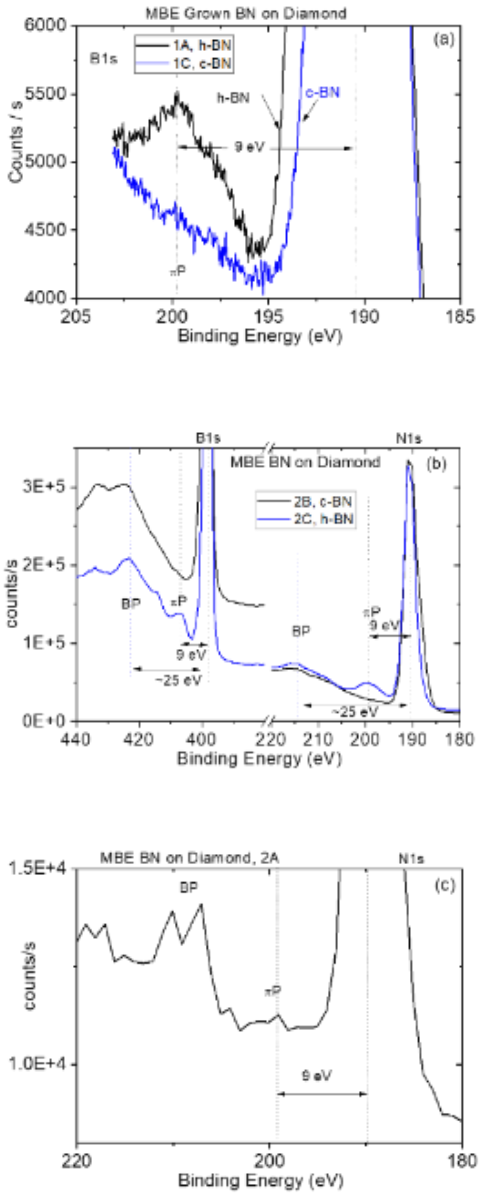

Fig. 11. XPS spectra of Samples 1A and 1C (a); 2B and 2C (b), and 2A (c). BP and πP indicate the positions of the bulk plasmon and π-plasmon, respectively. The presence of a small peak 9 eV above the B1s and N1s peak is indicative of the π-plasmon peak in h-BN; it is not found in c-BN [Ref. 16].

phase in FTIR. As indicated in Table 2, c-BN film growth occurred only when either the Mg cell was hot, or shortly after it had been hot and used for doping during a growth.

XPS confirmed the presence of B and N in the five samples, although sample 2A exhibited only weak B and N peaks. In addition, small peaks were observed in XPS at ~9eV higher energy than the B1s and N1s peaks in samples 1A and 2C as shown in Fig. 11. These peaks are consistent with π-plasmon peaks, which are indicative of sp^2 bonding. Hence, the appearance of these peaks in samples 1A and 2C, but not in 1C or 2B, is consistent with the phase identification by FTIR.

We hypothesize that even with the shutters closed and the Mg beam blocked, trace amounts of Mg are deposited on the diamond substrate via the "drag effect" described by Wasilewski, et al. in 1997 [19]. Likewise, re-evaporation of Mg deposited on the inside walls of the MBE chamber during a previous growth may lead to trace amounts of Mg adsorbing on the diamond substrate surface. Hence, even trace amounts of magnesium deposited on the diamond substrate surface appear to facilitate the growth of cubic boron nitride instead of the hexagonal phase. We estimate the probability that the results in Table 2 arise from random chance to be less than 0.4%.

On the basis of this observation, epitaxial growth of BN on diamond is now initiated with the co-deposition of ~0.005 monolayer-equivalent of Mg. Since this has been incorporated into the standard growth protocol, FTIR indicates that 8 of 10 samples grown are c-BN, the remainder being too thin to exhibit either cubic or hexagonal character. Hence, trace amounts of Mg deposited on the diamond surface at the initiation of growth greatly facilitates the subsequent growth of c-BN.

We speculate that this trace amount of Mg facilitates the nucleation of c-BN by locally melting the deposited sp^2-bonded BN, from which c-BN may more easily form and condense [19]. It is suggestive that Mg and Mg_3N_2 are known flux precursors in the conversion of h-BN to c-BN at high temperature and pressure [20, 21], and it may be that Mg acting in concert with energetic ions impinging on the growth surface performs a similar function. We also note that Bhaumik and

Narayan observed extensive twinning, similar to that observed in our Sample 4, in c-BN formed by pulsed laser annealing of h-BN films, in which the h-BN was melted by laser pulses and recrystallized as c-BN [22].

SUMMARY

Films of cubic boron nitride have been grown on diamond (001) substrates with rms surface roughness 0.5-2.5 nm and prepared either with a solvent degrease or with an aggressive acid clean which leaves the diamond surface oxygen-terminated. Films have been characterized by FTIR, XPS, and scanning transmission electron microscopy. Scanning TEM reveals epitaxial and textured films in which the c-BN (110) is parallel to the diamond (110), the film consists of >99% cubic phase, consistent with the results of FTIR, and the interface is structurally abrupt. Nearly all the visible defects are stacking faults, which occur with a high density. No intermediate layer is observed between the c-BN and the diamond; however, electron energy loss spectroscopy reveals the presence of sp^2-bonded BN at the interface, the film surface, and at isolated misfit dislocations.

Magnesium is shown to enable the growth of c-BN by ion beam-assisted MBE, even at trace amounts. Areal densities of $\sim 5 \times 10^{10}$ cm^{-2}, corresponding to 5×10^{-5} monolayer equivalent, are sufficient to enable c-BN growth on diamond.

Improvements in boron flux control are expected, and should result in improved film growth, film quality, growth rate uniformity, and control of dopant concentrations and profiles. These in turn will enable the correlation of electronic and optical properties of c-BN films to growth conditions and dopant concentrations, and will enable the growth of device structures such as *p-n* junctions.

REFERENCES

[1] H. Yin and P. Ziemann, Appl. Phys. Lett. **104**, 252111 (2014)
[2] http://www.ioffe.ru/SVA/NSM/Semicond/index.html
[3] B. He *et al.*, Appl. Phys Lett. **92**, 102108 (2008)
[4] O. Mishima *et al.*, Science **238**, 181 (1987)
[5] X. Guo *et al.*, Appl. Surf. Sci. **321**, 94 (2014)
[6] X. Yang and Q.-L. Ye, J. Alloys Comp. **580**, 1 (2013)
[7] D.V. Shtansky *et al.*, Sci. Technol. Adv. Mater. **1**, 219 (2000)
[8] K. Hirama *et al.*, Appl. Phys. Lett. **104**, 092113 (2014)
[9] K. Hirama *et al*., Appl. Phys. Express **10**, 035501 (2017)
[10] V.A. Gubanov *et al.*, Phys. Rev. B **56**, 13077 (1997)
[11] N. Izumskaya *et al.*, Adv. Electron. Mater. **3**, 1600485 (2017)
[12] X.W. Zhang, Thin Solid Films **544**, 2 (2013)
[13] H. Yin and P. Ziemann, Appl. Phys. Lett. **104**, 252111 (2014)
[14] T. Shimaoka, K. Ichikawa, S. Koizumi, K. Watanabe, and T. Teraji, Phys. status solidi, **216**, 1900247 (2019).

[15] S. Kono, T. Kageura, Y. Hayashi, S.-G. Ri, T. Teraji, D. Takeuchi, M. Ogura, H. Kodama, A. Sawabe, M. Inaba, A. Hiraiwa, H. Kawarada, Diam. Relat. Mater. **93**, 105 (2019)
[16] D.F. Storm, S.I. Maximenko, A.C. Lang. N. Nepal, T.I. Feygelson, B.B. Pate, C.A. Affouda, and D.J. Meyer, Phys. Status Solidi RRL (2022) doi: 10.1002/pssr.202200036
[17] P. Widmayer, H.G. Boyen, P. Ziemann, P. Reinke, and P. Oelhafen, Phys Rev B **59**, 5233 (1999)
[18] X.W. Zhang, H.-G. Boyen, N. Deyneka, P. Ziemann, F. Banhart, and M. Schreck, Nature Mater. **2**, 312 (2003)
[19] W. Wasilewsky, S.J. Rolfe, and R.A. Wilson, J. Cryst. Growth **175/176**, 1270 (1997)
[20] R. Trehan, Y. Lifshitz, and J.W. Rabelais, J. Vac. Sci. Technol., A **8**, 4026 (1990)
[21] L. Vel, G. Demazeau, and J. Etourneau, Mat. Sci. Engineer. **B10**, 149 (1991)
[22] A. Bhaumik and J. Narayan, Phys. Chem. Chem Phys. **21**, 1700 (2019)